

Transition from the Bose gas to the Fermi gas through a Nuclear Halo

V.P. Maslov *

Abstract

The first part of the paper deals with the behavior of the Bose–Einstein distribution as the activity $a \rightarrow 0$. In particular, the neighborhood of the point $a = 0$ is studied in great detail, and the expansion of both the Bose distribution and the Fermi distribution in powers of the parameter a is used.

This approach allows to find the value of the parameter a_0 , for which the Bose distribution (in the statistical sense) becomes zero.

In the second part of the paper, the process of separation of a nucleon from the atom’s nucleus is studied from the mathematical point of view. At the moment when the nucleon tears away from the fermionic nucleus, the nucleus becomes a boson. We investigate the further transformations of bosonic and fermionic separation states in a small neighborhood of the pressure P equal to zero. We use infinitely small quantities to modify the parastatistical distribution. Our conception is based on interpolation formulas yielding expansions in powers of the density. This method differs from those in other models based on the interaction potential between two or three particles.

We obtain new important relations connecting the temperature with the chemical potential during the separation of a nucleon from the atom’s nucleus. The obtained relations allow us to construct, on an antipode of sorts of the Hougen–Watson P-Z chart, the very high temperature isotherms corresponding to nuclear matter. It is proved mathematically that the passage of particles satisfying the Fermi–Dirac distribution to the Bose–Einstein distribution in the neighborhood of pressure P equal to zero occurs in a region known as the “halo”.

1 Statistical transition of the Bose gas to the Fermi gas

1.

It is well known that a Bose particle consists of two bound Fermi particles. For a Bose particle to become a Fermi particle, it is necessary that one of the Fermi particles forming the Bose particle must be “pushed out” *beyond* the volume V under consideration (in the two-dimensional case, V is the area) under the action of some energy. In the case of the volume of a ball (the area of a disk), the radius r is the radius of the “shell,” outside which the “entanglement” of two fermions into one boson terminates according to the Einstein–Podolsky–Rosen concept.

*National Research University Higher School of Economics, Moscow, 123458, Russia; Moscow State University, Physics Faculty, Moscow, 119234, Russia

Let there be given a macroscopic volume V of radius at least 1 mm filled completely with a Bose gas (for example, helium-4) for the activity $a = 1$, i.e., on the caustic. We shall determine what amount of energy is required to “push out” one fermion from the specific volume under consideration. To obtain the total energy, i.e., the energy needed for the Bose gas (for example, helium-4) to go over completely into the Fermi gas (for example, helium-3), we must multiply the resulting quantity by the number of particles in the gas. It is the amount of energy required for the transition of the Bose gas to the Fermi gas that is the subject of the present study. In particular, we shall show that, for the number of degrees of freedom $D > 2$, we will have a jump of the energy E at the point $E = 1/\log a$ for $a = 0$, where a is the activity,

Remark 1. “The barrier” formed by the shell is described by a Bardeen–Cooper–Schrieffer type equation for Cooper pairs [1]–[2]. Since the volume under consideration is macroscopic (at least 1 mm³), by statistical calculations, the shell far exceeds the volume of the nucleus.

In our conception, we use the polylogarithm. The polylogarithm is determined by the activity a and the number of degrees of freedom D , where $D = 2\gamma + 2$ and γ is an auxiliary parameter. In the two-dimensional case, $\gamma = 0$, while, in the general number theory, $\gamma \leq 0$. The positive value $\gamma > 0$ corresponds to the gas state in classical thermodynamics and $\gamma < 0$, to the liquid state.

Both parameters a and D are dimensionless, while the volume V is a dimensional parameter. The dimensionless small parameter

$$\frac{\hbar^2}{mVT} \quad (1)$$

for $\gamma = 0$ (in the two-dimensional case, V is the area) corresponds to the semiclassical approximation in the sense that the semiclassical asymptotics is expanded in terms of this parameter. Therefore, as a rule, a parameter λ is also added so that the multiplicative term before the polylogarithm becomes dimensionless. Statistical quantities divided by the number of particles i.e., belonging to one particle, are called *specific quantities*: V/N is the *specific volume* and E/N is the *specific energy*. We proceed as follows: first, we shall find the specific energy and, further, we shall multiply it by the number of particles on the caustic $a = 1$.

The quantity $PV/(NT)$, where P is the pressure and T is the temperature, is dimensionless. It is called the *compressibility factor*. The temperature T in the two-dimensional case is determined from the relation $M = T \operatorname{Li}_2(a)$, where $a = 1$, as

$$T = \sqrt{\frac{M}{\zeta(2)}}, \quad (2)$$

where $\zeta(\cdot)$ is the Riemann zeta-function.

For the number of degrees of freedom $D > 2$, the density of the Bose gas at the point $a = 0$ vanishes as $1/|\log a|$ and behaves as $1/\log a$ for the Fermi gas (see below), just as the energy E of the Bose gas. The coefficient of $1/\log a$ for the energy of the Bose gas allows us to determine the energy needed for “all” the Bose particles to go over into Fermi particles.

The hidden parameter appearing in the Einstein–Podolsky–Rosen paradox could unite quantum and classical mechanics in the sense defined by the author; it can be obtained from the general arguments in the first chapter of the book [3]. After Sec. 4 “Role of Energy,” the most important notion of time is introduced in Sec. 5 “Statistical Matrix.” Since, in the present paper, we calculate the statistical energy ΔE required for the transition of the Bose

gas into the Fermi gas, it follows that by using Sec. 5 of the book [3] we can also calculate the statistical time

$$\Delta t \sim \frac{\hbar}{\Delta E}, \quad (3)$$

given by the authors of [3] to explain the transition to macroscopic physics. From the point of view of the metamathematical hidden parameter, this time plays a role similar to that of the mean free time in classical mechanics.

Let k denote the maximal admissible number of particles that can occupy one energy level, and let N_i denote the number of particles located at the i th energy level ¹. The number k is the maximal number of particles located at one energy level of a quantum operator of the Hamiltonian \hat{H} . For a Bose systems, it is obvious that $N_i \leq N$. Therefore, for a Bose system, $k \leq N$.

On the other hand, the number N_i is arbitrarily large, more precisely, maximally large, in view of the inequality $N_i \leq N$. This implies that $k = N$, and we obtain an equation for N in which, on the left-hand and right-hand sides, we have N from the formula for the Gentile parastatistics (see Sec. 4 below).

2. To find the energy that is of interest to us (the energy of transition of Bose particles to Fermi particles), it suffices to study the transition at the point $a = 0$. If we wish to widen the interval of the jump from the Bose distribution to the Fermi distribution, then we must use parastatistics, or Gentile statistics [6] in which the first term in parentheses gives the distribution for Bose particles and the other term, the parastatistical correction. The corresponding formula in the three-dimensional case is of the form (see [7])

$$N = \lambda \left\{ \int_0^\infty \frac{p^2 dp}{\exp\{p^2/2mT\} - 1} - (k+1) \int_0^\infty \frac{p^2 dp}{\exp\{(k+1)p^2/2mT\} - 1} \right\}. \quad (4)$$

For the Bose–Einstein distribution in the case of D degrees of freedom the following formulas are valid:

$$E = T\Phi(\gamma+1)Li_{2+\gamma}(a), \quad N = \Phi Li_{1+\gamma}(a). \quad (5)$$

Here and elsewhere, $\gamma = D/2 - 1$, T is the temperature, $a = e^{\mu/T}$ is the activity, μ is the chemical potential,

$$\Phi = \left(\frac{\sqrt{2\pi mT}}{2\pi\hbar} \right)^{2(\gamma+1)} V,$$

where m is the mass of one particle, V is the volume of the system of particles, and \hbar is the Planck constant.

For the Fermi–Dirac distribution, the following formulas hold:

$$E = -T\Phi(\gamma+1)Li_{2+\gamma}(-a), \quad N = -\Phi Li_{1+\gamma}(-a). \quad (6)$$

As we see, formulas (5) and (6) differ by sign; therefore, the activity a passes through the point $a = 0$.

In the case of parastatistics, i.e., there are at most k particles at each level, the following relations hold:

$$E = \Phi T(\gamma+1) \left(Li_{2+\gamma}(a) - \frac{1}{(k+1)^{\gamma+1}} Li_{2+\gamma}(a^{k+1}) \right), \quad (7)$$

$$N = \Phi \left(Li_{1+\gamma}(a) - \frac{1}{(k+1)^\gamma} Li_{1+\gamma}(a^{k+1}) \right). \quad (8)$$

¹For the transition from a discrete spectrum to a continuous one with respect to the parameter V , see [4], [5].

According to the conventional definitions, for $k = 1$, we have the Fermi case and, for $k = \infty$, the Bose case.

Let us consider another important dimensionless quantity, which was mentioned above, namely, the compressibility factor defined by the formula $Z = PV/NT$.

The following thermodynamic relation is well known:

$$E = -(\gamma + 1)\Omega = PV(\gamma + 1) \quad (9)$$

As is seen from relation (9), PV is expressed in terms of E ; therefore, the compressibility factor can be expressed in terms of the polylogarithm. For the Bose case, the compressibility factor takes the form

$$Z|_{\text{Bose}} = \frac{Li_{2+\gamma}(a)}{Li_{1+\gamma}(a)} \quad (10)$$

and, for the Fermi case, we have

$$Z|_{\text{Fermi}} = \frac{Li_{2+\gamma}(-a)}{Li_{1+\gamma}(-a)}. \quad (11)$$

For the Gentile statistics with parameter k , we have the following expression for the compressibility factor:

$$Z|_k = \frac{Li_{2+\gamma}(a) - \frac{1}{(k+1)^{\gamma+1}} Li_{2+\gamma}(a^{k+1})}{Li_{1+\gamma}(a) - \frac{1}{(k+1)^\gamma} Li_{1+\gamma}(a^{k+1})}. \quad (12)$$

3. The compressibility factor Z multiplied by the temperature T is the specific energy. To obtain the jump of the specific energy, it suffices to consider the jump of the compressibility factor from the Fermi system to the Bose system.

The following representation for the polylogarithm is known:

$$Li_s(a) = \sum_{i=1}^{\infty} \frac{a^i}{i^s}; \quad (13)$$

substituting this expression into (10), (11), (12), we obtain the following expansions of the compressibility factor:

$$\begin{aligned} Z|_{\text{Fermi}} &= 1 + a2^{-\gamma-2} - a^2 2^{-2\gamma-3} 3^{-\gamma-2} (2^{2\gamma+4} - 3^{\gamma+2}) \\ &\quad - a^3 2^{-3\gamma-4} 3^{-\gamma-2} (7 \cdot 2^{2\gamma+2} - 3^{\gamma+2} - 2^\gamma 3^{\gamma+3}) \\ &\quad - a^4 2^{-4\gamma-5} 3^{-2\gamma-3} 5^{-\gamma-2} (2^{4\gamma+7} 3^{2\gamma+3} - 2^{4\gamma+6} 5^{\gamma+2} - 3^{2\gamma+3} 5^{\gamma+2} + 2^{2\gamma+3} 3^{\gamma+1} 5^{\gamma+3} - 2^\gamma 3^{2\gamma+3} 5^{\gamma+3}) \\ &\quad + O(a^5), \end{aligned} \quad (14)$$

$$\begin{aligned} Z|_{\text{Bose}} &= 1 - a2^{-\gamma-2} - a^2 2^{-2\gamma-3} 3^{-\gamma-2} (2^{2\gamma+4} - 3^{\gamma+2}) \\ &\quad + a^3 2^{-3\gamma-4} 3^{-\gamma-2} (7 \cdot 2^{2\gamma+2} - 3^{\gamma+2} - 2^\gamma 3^{\gamma+3}) \\ &\quad - a^4 2^{-4\gamma-5} 3^{-2\gamma-3} 5^{-\gamma-2} (2^{4\gamma+7} 3^{2\gamma+3} - 2^{4\gamma+6} 5^{\gamma+2} - 3^{2\gamma+3} 5^{\gamma+2} + 2^{2\gamma+3} 3^{\gamma+1} 5^{\gamma+3} - 2^\gamma 3^{2\gamma+3} 5^{\gamma+3}) \\ &\quad + O(a^5). \end{aligned} \quad (15)$$

The jump of the compressibility factor is expressed as (see Fig. 1):

$$\Delta Z(a) = Z|_{K=1} - Z|_{\text{Bose}} = \frac{a}{2^{\gamma+1}} + O(a^2), \quad (16)$$

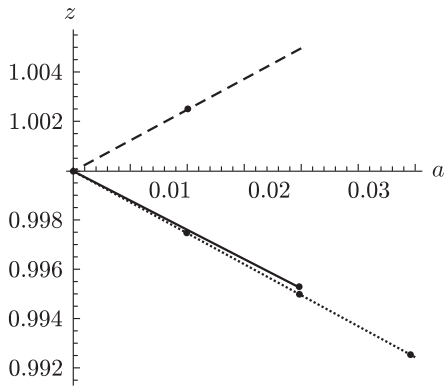


Figure 1: Dependence of the compressibility factor Z on the activity a for the two-dimensional case. Here $\Phi = 100$, $\gamma = 0$. The upper (dashed) curve corresponds to the Fermi system. The middle (solid) curve corresponds to the Bose system up to $O(a^2)$. The lower (dotted) curve corresponds to the exact Bose system. The points on the curves correspond integer N .

while the jump of the *specific* energy E_{spec} is of the form

$$\Delta E_{\text{spec}}(a) = T(\gamma + 1)\Delta Z(a) = T(\gamma + 1)\frac{a}{2^{\gamma+1}} + O(a^2). \quad (17)$$

The dependence of the compressibility factor Z on the activity a for the case $\gamma = 0$ is shown in Fig. 1.

4. As indicated above, the author obtained a self-consistent equation in which N is an unknown quantity. We are interested in the point at which the number of Bose particles N is 0, i.e., the point at which Bose particles vanish. An example of this point is given in Fig. 2. Let us note that the value of the activity a is not zero at this point; it depends essentially on the function Φ and the parameter γ . Let us consider successively the cases of small N , $\gamma \geq 0$, and $\gamma < 0$.

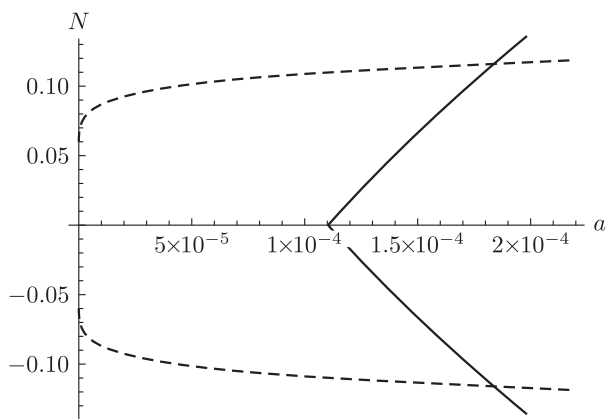


Figure 2: Dependence $N(a)$ for $W = 1000$, where $W = V(\lambda^2 T)^{\gamma+1}$, λ is the parameter depending on the mass, and $\gamma = 0$. The dotted curve corresponds to $N = -1/\log(a)$. The sold line corresponds to $N = 0$.

4.1. As pointed out above, there can be at most N particles at each energy level. Therefore, for the Bose system, we put $k = N$. Equation (8) takes the form:

$$N = \Phi(Li_{1+\gamma}(a) - \frac{1}{(N+1)^\gamma} Li_{1+\gamma}(a^{N+1})). \quad (18)$$

Expanding the right-hand side of Eq. (18) in the small parameter $N \ll a$, we obtain

$$N = \Phi N(\gamma \text{Li}_{\gamma+1}(a) - \log(a) \text{Li}_{\gamma}(a)) + \frac{1}{2} W N^2 (\log^2(a) (-\text{Li}_{\gamma-1}(a)) - \gamma((\gamma+1) \text{Li}_{\gamma+1}(a) - 2 \log(a) \text{Li}_{\gamma}(a))) + o((\log a N)^2). \quad (19)$$

Remark 2. We deal with two double limits. The first case is

$$\lim_{a \rightarrow 0} a \lim_{N \rightarrow 0} N.$$

In this case, $N \ll a$, and we obtain some value of a_0 for which the number of Bose particles of the distribution $N = 0$.

In the second case, N is fixed and $a \ll N$. As a result, the Gentile parastatistical term vanishes.

If, in the expansion (18), we take into account the terms up to the second order of smallness inclusive, then we can obtain the equation for N whose solution is as follows:

$$N = 2 \frac{\gamma \Phi \text{Li}_{\gamma+1}(a) - \Phi \log(a) \text{Li}_{\gamma}(a) - 1}{\Phi (\log^2(a) \text{Li}_{\gamma-1}(a) + \gamma((\gamma+1) \text{Li}_{\gamma+1}(a) - 2 \log(a) \text{Li}_{\gamma}(a)))}. \quad (20)$$

Equation (20) yields the following equation for a_0 in the case $N = 0$:

$$\gamma \Phi \text{Li}_{\gamma+1}(a_0) - \Phi \log(a_0) \text{Li}_{\gamma}(a_0) - 1 = 0, \quad (21)$$

For small a_0 , the following asymptotic formula holds:

$$\Phi = -\frac{1}{a_0 \ln a_0}, \quad (22)$$

or

$$\Phi = \frac{1}{a_0 \ln \Phi}. \quad (23)$$

We obtain

$$\Delta Z(a_0) = \frac{a_0}{2^{\gamma+1}} = -\frac{1}{2^{\gamma+1} \Phi \ln a_0}. \quad (24)$$

The maximal number of particles N_c in the system is at the caustic point $a = 1$. The value of N_c is given by

$$N_c = \Phi (Li_{1+\gamma}(1) - \frac{1}{(N_c + 1)^{\gamma}} Li_{1+\gamma}(1)). \quad (25)$$

We shall use the integral representation of the polylogarithm Li , obtaining

$$N_c = \Phi \beta \int_0^{\infty} \left(\frac{1}{\exp\{\varepsilon/T\} - 1} - \frac{N_c + 1}{\exp\{(N_c + 1)\varepsilon/T\} - 1} \right) d\varepsilon, \quad \beta = 1/T. \quad (26)$$

4.2. Consider the case $D = 2$. Let $N = N_c$ be the solution of Eq. (26). We shall evaluate the integral in (26) (with the same integrals) taken from δ to ∞ and then pass to the limit as

$\delta \rightarrow 0$. After making the change $\beta x = \xi$ in the first term and $\beta(N_c + 1)x = \xi$ in the second term, where $\beta = 1/T$, we obtain

$$N_c = \Phi \int_{\delta\beta}^{\infty} \frac{d\xi}{e^\xi - 1} - \Phi \int_{\delta\beta(N_c+1)}^{\infty} \frac{d\xi}{e^\xi - 1} + O(\delta) = \Phi \int_{\delta\beta}^{\delta\beta(N_c+1)} \frac{d\xi}{e^\xi - 1} + O(\delta) \quad (27)$$

$$\sim \Phi \int_{\delta\beta}^{\delta\beta(N_c+1)} \frac{d\xi}{\xi} + O(\delta) = \Phi \{\ln(\delta\beta(N_c + 1)) - \ln(\delta\beta)\} + O(\delta) = \Phi \ln(N_c + 1) + O(\delta). \quad (28)$$

In the three-dimensional case, this formula is of the form (4).

After passing to the limit as $\delta \rightarrow 0$, we obtain

$$N_c = \Phi \log(N_c + 1). \quad (29)$$

Multiplying the difference of the specific energies $\Delta E_{\text{spec}}(a_0)$ by the number of particles defined by formula (25), we obtain the difference of the energies for the whole system of particles in the units of T in the case $\gamma > 0$:

$$\Delta E = \Delta E_{\text{spec}}(a_0) N_c = \frac{\gamma + 1}{2^{\gamma+1} \ln \Phi} Li_{1+\gamma}(1) \left(1 - \frac{1}{(N_c + 1)^\gamma}\right) \quad (30)$$

and, in the case $\gamma = 0$, we have

$$\Delta E = \Delta E_{\text{spec}}(a_0) N_c = \frac{1}{2 \ln \Phi} \log(N_c + 1), \quad (31)$$

where N_c can be calculated from formula (25) (which contains Φ).

4.3. Let us pass to the case $\gamma < \gamma_0 < 0$, i.e., $D < D_0 < 2$.

For the case in which $\gamma < \gamma_0 < 0$, the following lemma holds.

Lemma 1. *Consider the integral*

$$N = B \int_0^\infty \left(\frac{1}{e^{\beta x - \beta \mu} - 1} - \frac{k}{e^{k(\beta x - \beta \mu)} - 1} \right) x^\gamma dx, \quad (32)$$

where $-1 < \gamma < \gamma_0 < 0$, and $B > 0$ and $k > 0$ are constants.

Then

$$N = -\frac{B}{\beta^{\gamma+1}} c_{\beta\mu,\gamma} + \frac{Bk^{-\gamma}}{\beta^{\gamma+1}} c_{k\beta\mu,\gamma}, \quad (33)$$

where

$$c_{\mu,\gamma} = \int_0^\infty \left(\frac{1}{\xi - \mu} - \frac{1}{e^{\xi - \mu} - 1} \right) \xi^\gamma d\xi. \quad (34)$$

By the Lemma, Eq. (19) takes the form

$$N_c = \Phi C(\gamma) (-1 + (N_c + 1)^{-\gamma}), \quad (35)$$

where

$$C(\gamma) = \frac{1}{\Gamma(\gamma + 1)} \int_0^\infty \left(\frac{1}{\xi} - \frac{1}{e^\xi - 1} \right) \xi^\gamma d\xi. \quad (36)$$

As $N_c \rightarrow \infty$, we can neglect the summand -1 in formula (35) as well as 1 compared to N_c , whence we obtain

$$N_c = \Phi C(\gamma) N_c^{-\gamma}, \quad (37)$$

$$N_c = (\Phi C(\gamma))^{1/(\gamma+1)} = T \left(\left(\frac{\sqrt{2\pi m}}{2\pi\hbar} \right)^{2(\gamma+1)} VC(\gamma) \right)^{1/(\gamma+1)}; \quad (38)$$

as a final result, we arrive at the expression

$$N_c = T(VC(\gamma))^{1/(\gamma+1)} \left(\frac{\sqrt{2\pi m}}{2\pi\hbar} \right)^2. \quad (39)$$

For the jump of the energy, we obtain the expression

$$\Delta E = \frac{\gamma + 1}{2^{\gamma+1} \Phi \ln \Phi} (\Phi C(\gamma))^{1/(\gamma+1)} = \frac{\gamma + 1}{2^{\gamma+1} \ln \Phi} C(\gamma)^{1/(\gamma+1)} \Phi^{-\gamma/(\gamma+1)}. \quad (40)$$

2 Using infinitesimal quantities to describe the separation process of neutrons from atomic nuclei

A Bose particle consists of two Fermi particles which are linked together by an interaction force or, as it is customary to say at the present time, by an entangling force. Sometimes the two fermions constituting the boson are absolutely identical. They cannot be distinguished or numbered. Sometimes the fermions differ in mass, then they can be distinguished. For example, a proton and an electron are fermions of different mass, and together they constitute a pair – a boson. Such fermions can be distinguished and numbered, using the mechanism of numeration theory. While if the masses of the particles approach each other and coincide in the limit, then we cannot distinguish them.

The passage from the case of distinguishable particles to the case when the particles become undistinguishable leads to other quantum-mechanical formulas and therefore, to different commutation relations [8].

The separation of a fermion from the nucleus and the capture of a fermion is a very rapid process. The question of the possibility of monitoring that transformation as if it occurred in slow motion arises. Mathematically, this means that we must use such tools which may be applied to both fermions and bosons.

In the present paper we use infinitely small quantities to modify the parastatistical distribution (the Gentile statistical method). This approach allows to apply the “antipod” of the P-Z chart corresponding to the Van-der-Waals equation of state in thermodynamics, also known as the Hougen–Watson chart. In this antipode, the isotherms under consideration, unlike those in the Van-der-Waals model, correspond to extremely high temperatures, which increase even more when the compressibility factor Z decreases.

The obtained antipode of the P-Z chart adequately corresponds to the behavior of nuclear matter. We will show in this paper that the passage of particles satisfying the Fermi–Dirac distribution to the Bose–Einstein distribution in the neighborhood of pressure P equal to zero occurs in a region known as the “halo”. This region is different for various isotopes and depends on chemical potentials.

The method developed in this paper differs from those in other models based on the interaction of two or three particles, such as the Faddeev–Skyrme model or models involving the Lennard–Jones potential. This method is based on interpolation formulas yielding

expansions in powers of the density. Just as in the Van-der-Waals interpolation formula, the zeroth approximation is given by ideal gas, whereas in models based on potentials the zeroth approximation is given by the zero potential.

Niels Bohr in 1936 proposed one of the earliest models of the atomic nucleus in the framework of the theory of compound nucleus [9]. Later, by Carl Weizsäcker was obtained a semi-empirical formula for the binding energy of the atomic nucleus E_c :

$$E_c = \alpha A - \beta A^{2/3} - \gamma \frac{Z^2}{A^{1/3}} - \varepsilon \frac{(A/2 - Z)^2}{A} + \delta, \quad (41)$$

where

$$\delta = \begin{cases} +\chi A^{-3/4} & \text{for even-even nuclei,} \\ 0 & \text{for nuclei with odd } A, \\ -\chi A^{-3/4} & \text{for odd-odd nuclei,} \end{cases}$$

A is the mass number (total number of nucleons) in the nucleus, Z is the charge number (number of protons) in the nucleus, and α , β , γ , ε , and χ are parameters obtained by statistical treatment of experimental data. This formula provides sufficiently exact values of the binding energies and masses for many nuclei, which permits using it to analyze different properties of the atomic nucleus.

In this paper we obtain new important relations between the temperature and the chemical potential in the process of nucleon separation from the atomic nucleus. For this, we use the parastatistic relations modified by the mathematical notion of infinitesimals.

2.1 New parastatistics

Let us assume that the energy of each of the particles takes one of the values of the given discrete spectrum. We shall denote by N_i the number of particles located at the i -th level energy.

Besides the Bose–Einstein and Fermi–Dirac statistics, physicists use parastatistics (aka Gentile statistics [6]) that generalizes the two previously mentioned statistics, which are thus particular cases of parastatistics. According to the latter, as it was said earlier, at each energy level, there may be no more than K particles. By the usual definitions, the Fermi case is realized for $K = 1$. In the case of Bose statistics $N_i \leq N$ because then $\sum_i N_i = N$, implies that $K = N$.

We will be dealing with infinitely small K and N equal to each other. General approach see in [10].

In the case of parastatistics, we have the following relations, in which the first term in parentheses gives the distribution for Bose particles, and the second term, the parastatistical correction (compare (7)-(8)):

$$E = \frac{V}{\lambda^D} T(\gamma + 1) \left(\text{Li}_{2+\gamma}(a) - \frac{1}{(K + 1)^{\gamma+1}} \text{Li}_{2+\gamma}(a^{K+1}) \right), \quad (42)$$

$$N = \frac{V}{\lambda^D} \left(\text{Li}_{1+\gamma}(a) - \frac{1}{(K + 1)^\gamma} \text{Li}_{1+\gamma}(a^{K+1}) \right), \quad (43)$$

where $\text{Li}_{(\cdot)}(\cdot)$ is the polylogarithm function, $a = e^{\mu/T}$ is the activity (μ being the chemical potential, T being the temperature), $\gamma = D/2 - 1$, D is the number of degrees of freedom (the dimension), λ is the de Broglie wavelength:

$$\lambda = \sqrt{\frac{2\pi\hbar^2}{mT}}, \quad (44)$$

where \hbar is the Planck constant, m the mass of one particle.

The de Broglie wavelength is related to the Bohr–Sommerfeld quantization condition, i.e., to the quantization of the angular momentum (see [11] and related works, in particular [12]–[18]).

2.2 Passage from the Bose-type region to the Fermi-type region through a nuclear halo

Before completely separating from a nucleus, a nucleon stays within an area around a nucleus where it is bound to a nucleus with entanglement forces. In this area the probability to discover a neutron is higher than the probability to discover a proton. It is well-known that the area where the density distribution of neutrons much exceeds the density distribution of protons is called a nuclear halo.

The region corresponding to the difference of pressure $P = 0$ and to an infinitely small sequence $\{P_K\} \rightarrow 0$ constitutes the nuclear halo. The passage from the Bose-type region to the Fermi-type region occurs through the nuclear halo, which contains the value of the pressure $P = 0$. We denote by a_0 the maximal value of the activity a for Bose particles as $N \rightarrow 0$. The quantity a_0 indicates the maximal value of the activity at which the decomposition of bosons into fermion occurs.

Let us recall some definitions and relationships that we used in the paper [19]. It will be helpful to consider more general cases later in this work.

For an ideal gas of dimension $D = 3$, relations (42), (43) become

$$N = \frac{V}{\lambda^3} (\text{Li}_{3/2}(a) - \frac{1}{(K+1)^{1/2}} \text{Li}_{3/2}(a^{K+1})), \quad (45)$$

$$E = \frac{3V}{2\lambda^3} T (\text{Li}_{5/2}(a) - \frac{1}{(K+1)^{3/2}} \text{Li}_{5/2}(a^{K+1})). \quad (46)$$

The expansion of the summand $\frac{1}{(K+1)^{1/2}} \text{Li}_{3/2}(a^{K+1})$ from formula (45) in small values of K has the form:

$$\frac{1}{(K+1)^{1/2}} \text{Li}_{3/2}(a^{K+1}) = \text{Li}_{3/2}(a) - [K(\text{Li}_{3/2}(a)/2 - \log(a) \text{Li}_{1/2}(a)) + O(K^2)]. \quad (47)$$

Let $B = V/\lambda^3 > 0$. Then equation (45) for small K acquires the form:

$$N = BK \left(\frac{1}{2} \text{Li}_{3/2}(a) - \log(a) \text{Li}_{1/2}(a) \right) + O(K^2). \quad (48)$$

In our considerations N is an infinitely small number, .. $N = \alpha_i$, where a sequence of infinitesimals $\alpha_i \rightarrow 0$ as $i \rightarrow \infty$. Similarly $K = \beta_i$, where a sequence of infinitesimals $\beta_i \rightarrow 0$ as $i \rightarrow \infty$. The sequences α_i and β_i are similar to each other, i.e. $\lim_{i \rightarrow \infty} \frac{\alpha_i}{\beta_i} = 1$. Thus we are not dealing with the Fermi statistics or the Bose statistics, but with a parastatistics of a new type, which can be called a Bose-like statistics.

Dividing both sides of (48) by N and taking the limit as $K \rightarrow 0$, yields an expression for a_0 , i.e., the value of a for which $K = N = 0$:

$$\frac{1}{2} \text{Li}_{3/2}(a_0) - \log(a_0) \text{Li}_{1/2}(a_0) - B^{-1} = 0. \quad (49)$$

Equation (49) in the case of an arbitrary coefficient $\gamma = D/2 - 1$ instead of $1/2$, after similar arguments, acquires the form:

$$\gamma \operatorname{Li}_{\gamma+1}(a_0) - \log(a_0) \operatorname{Li}_{\gamma}(a_0) - \frac{\lambda^{2(\gamma+1)}}{V} = 0. \quad (50)$$

Equation (50) has a unique solution $a_0 > 0$ that depends on B and γ .

In the case $K = N$, equation (45) acquires the form

$$N = B(\operatorname{Li}_{3/2}(a) - \frac{1}{(N+1)^{1/2}} \operatorname{Li}_{3/2}(a^{N+1})). \quad (51)$$

This equation obviously has the solution $N \equiv 0$ for any $a \geq 0$. However, for $a > a_0$, it has one more nonnegative solution $N(a)$. This can be verified by constructing the graphs of the right-hand and left-hand sides of (51) as a function of a for an arbitrary fixed $N > 0$. The right-hand side of the equation is zero for $a = 0$ and monotonically grows for $a \in (0, \infty)$, while the left hand side is a constant that does not depend on a .

Substituting the obtained relation $N(a)$ in formula (46), we can find the dependence $E(a)$, and with it the pressure $P(a)$, by using the relation

$$E = (\gamma + 1)PV. \quad (52)$$

Let us substitute the obtained relation into the graph of the compressibility factor

$$Z = PV/(NT) \quad (53)$$

as a function of P (this graph is known as the Hougén–Watson chart).

Now we place a minus sign before dependencies $P(a)$ and $N(a)$ for the Bose branch, i.e. these values are considered as negative. It follows from this that in the Bose-like region $Z(a) > 0$.

For Fermi statistics in the case $D = 3$, we have the relations

$$N = -\frac{V}{\lambda^3} \operatorname{Li}_{3/2}(-a), \quad (54)$$

$$E = -\frac{3}{2} \frac{V}{\lambda^3} T \operatorname{Li}_{5/2}(-a). \quad (55)$$

Let us call the curve on the P-Z chart, constructed according to formulas (54)–(55) of Fermi statistics, the Fermi branch. The pressure P , as well as the number of particles N , on the Fermi branch is positive.

2.3 Construction of the isotherm for nuclear matter

The value of the activity a for a known value of the temperature T determines the corresponding value of the chemical potential

$$\mu = T \log(a). \quad (56)$$

In particular, for $a = a_0$, the higher the temperature, the smaller is a_0 , and the larger is the value of $|\mu_0|$. Thus, as the temperature grows, the point of passage μ_0 approaches the point $\mu = -\infty$ at which the pressure P changes sign (see [20]).

The table 1 in Appendix presents values of a_0 and $\mu_0 = T \log a_0$ for isotopes of various chemical elements.

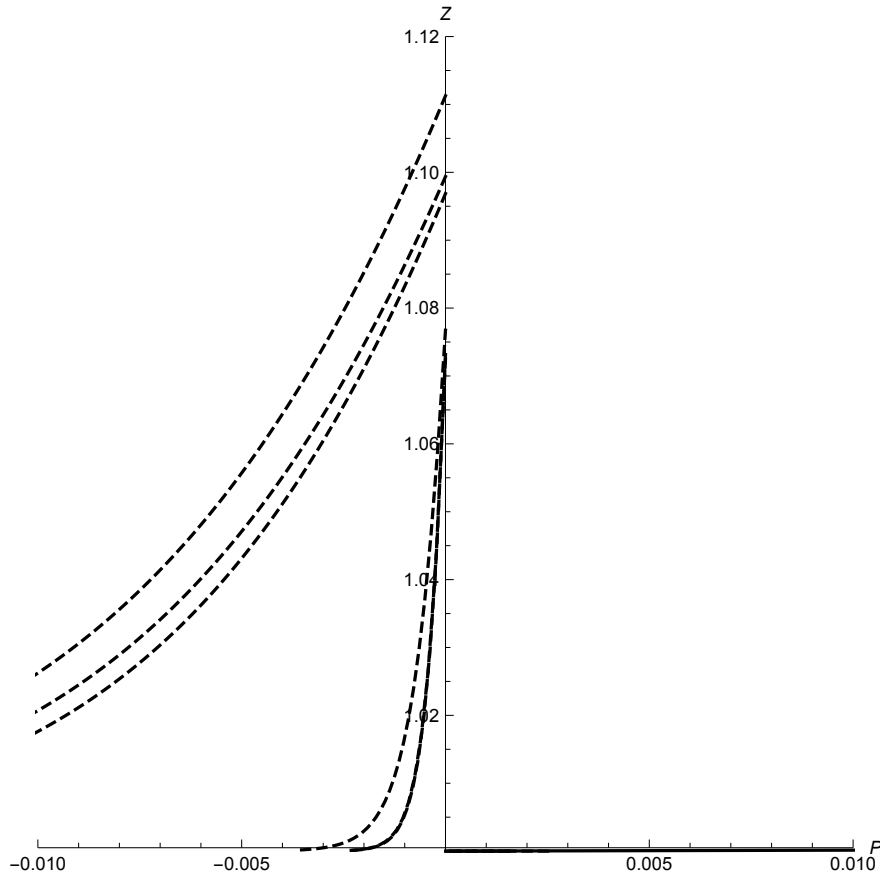


Figure 3: Dependence of the compressibility factor Z on the pressure P , expressed in the units MeV/fm^3 for argon-40, chromium-50, iron-54, lead-208, copernicium-285, Uup-290 (from top to bottom). The continuous line represents the line $Z = 1$. It is the beginning of the Fermi branch. The hashed lines show isotherms of the Bose branch, constructed according to formulas (45)–(46). The temperature is equal to the energy needed for the separation of the neutron B_{nExp} . The corresponding values of B_{nExp} and a_0 are given in Table 1 in Appendix.

The value of a_0 in the case of separation can be found by means of formula (49), taking into account the expression of the de Broglie wavelength λ in terms of the volume V of the nucleus, its temperature T and its mass m . The volume of the nucleus is taken to be that of a ball of radius $r_0 = A^{1/3}1.2 \times 10^{-15} \text{ m}^3$. The temperature T of the nucleus expressed in energy units is taken equal to the energy of separation of a neutron B_{nExp} (obtained from the database IsotopeData).

We have obtained an equation (49) from which we can find the value of a_0 , and can determine the temperature T at which this value is attained.

Fig. 3 shows the dependence of the compressibility factor $Z = PV/(NT)$ on the pressure P , expressed in the units MeV/fm^3 for argon-40, chromium-50, iron-54, lead-208, copernicium-285, and Uup-290. The dashed lines are the isotherms of the Bose branch constructed by means of formulas (45), (46), (53), and (52). The isotherms are parametric curves $P(a)$, $Z(a)$.

Let $\{P_K\}$ be an infinitely small sequence, coinciding with the infinitely small quantity K . It can be shown that the corresponding sequence $\{Z_k\}$ tends to a number greater than unity in the Bose-like region and to unity in the Fermi-like region (see Fig. 3).

The temperature is equal to the extremal value of the separation energy of the neutron

B_{nExp} , indicated in table 1. To each value of a_0 there corresponds a definite value of the temperature T . In turn, to each value of T there corresponds an isotherm on the Hougen–Watson chart. These isotherms lie in the second quadrant. If the volume is constant, the temperature characterizing the isotherm becomes smaller as the point $a = a_0$ becomes nearer to $a = 1$.

Thus we can say that the Van-der-Waals isotherms are in a sense opposite to the isotherms of nuclear matter shown in Fig. 3.

This shows that the chemical potential μ at $P = 0$ does not become equal to minus infinity and so the axis Z at $P = 0$ is not the boundary between two unrelated structures. Since the value of $|\mu_0|$ is very large but not infinite between the values of the infinitely small quantities $\{P_K\}$ and the region obeying the Fermi–Dirac distribution, there is a “halo” dividing the Bose region from the Fermi region.

The value of the chemical potential μ_0 determines the halo width. The halo expands as μ_0 is close to zero. It can become infinitely large. For example, one can see from Table 1 in Appendix, for values of μ_0 of order -100 the halo is relatively small, for μ_0 of order -80 the halo grows, for μ_0 of order -8 the halo becomes very large, and for μ_0 of order -0.4 the halo can be considered as infinite (e.g. berillium-9).

In the classical thermodynamics this situation corresponds to passing through the point where the pressure vanishes (i.e. passing from a negative compressibility factor Z to a positive Z). The halo is a domain of indeterminacy: nobody knows what happens with the particles in the domain of a nuclear halo. We can refer to halo as the lacunary indeterminacy.

We do not consider the problem of proving that the isotherms on Fig. 3 exist. We give an approximate solution of the obtained equations (see similar approaches in papers [21], [22]), in which all the isotherms corresponding to different values of a_0 are approximately constructed.

In the point $a = 1$ (i.e. on the spinodal) the compressibility factor has the form:

$$Z_s = \frac{\zeta(5/2)}{\zeta(3/2)} \frac{1 - \frac{1}{(N_s+1)^{3/2}}}{1 - \frac{1}{(N_s+1)^{1/2}}}, \quad (57)$$

where N_s is determined from the relation

$$N_s = \frac{V}{\lambda^3} \zeta(3/2) \left(1 - \frac{1}{(N_s + 1)^{1/2}} \right). \quad (58)$$

In the Fig. 4 upper ends of isotherms correspond to $a = a_0$. In the Fig. 3 corresponding points lie on the axis Z . This makes it possible to consider and compare behavior of isotherms of different chemical elements. In Fig. 5 isotherms shown in Fig. 3 are drawn on a different scale.

One can see in Fig. 5 that the tangent to the lead curve in the bend point is parallel to the axis Z . This is a very important point where the activity $a = 1$. It connects the matter under consideration with the Van-der-Waals gas. This point is evidence of passing to the nuclear matter. Nuclear matter is a substance which in contrast to the nucleus has no boundaries. The bending down of the lead isotherm indicates that in the separation process of neutrons from an atomic nuclei we pass to another substance of nuclear matter.

Thus we have described a complete picture of passing from a substance which occurs when a neutron separates from an atomic nucleus to the nuclear matter substance.

Conclusion

We have shown that using infinitesimals N and K equally fast tending to zero leads to the determination of the value of a parameter a_0 that allows us to construct an antipode of sorts

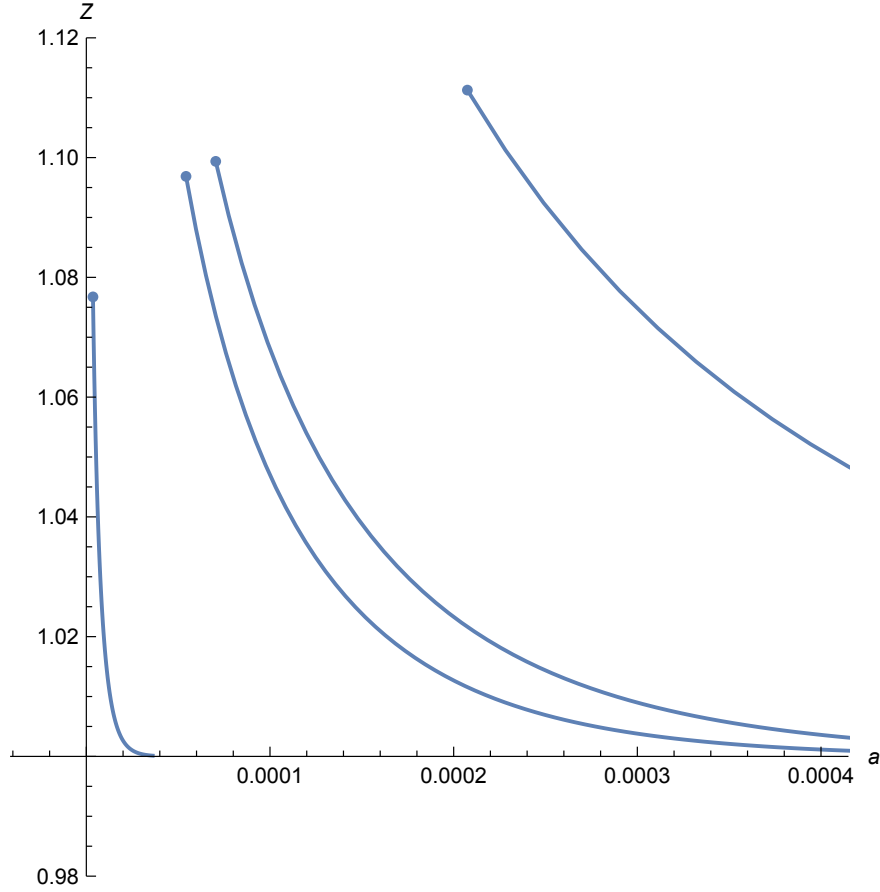


Figure 4: Dependence of the compressibility factor Z on the activity a , expressed in the units MeV/fm^3 for lead-208, iron-54, chromium-50, argon-40 (from left to right). The lines show isotherms of the Bose branch, constructed according to formulas (45)–(46). The temperature is equal to the energy needed for the separation of the neutron B_{nExp} (see Table 1 in Appendix).

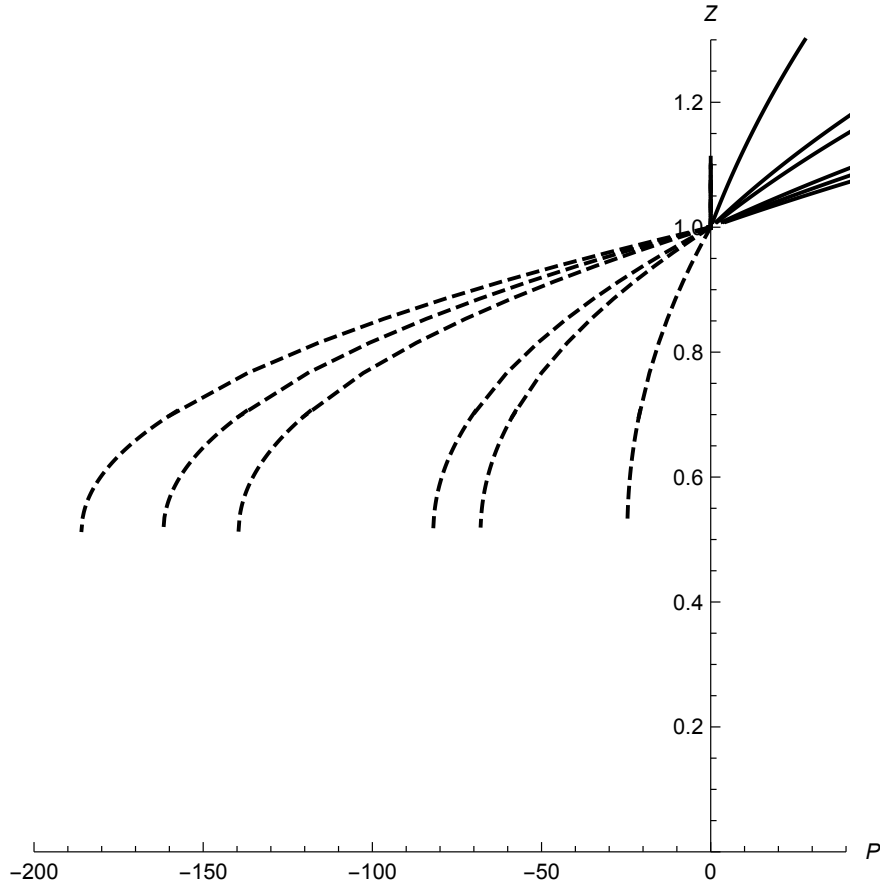


Figure 5: Dependence of the compressibility factor Z on the pressure P , expressed in the units MeV/fm^3 for Uup-290, copernicium-285, lead-208, iron-54, chromium-50, argon-40, (from left to right in the region $P \leq 0$). The continuous line represents the Fermi branch. The hashed lines show isotherms of the Bose branch, constructed according to formulas (45)–(46). The temperature is equal to the energy needed for the separation of the neutron B_{nExp} (see Table 1 in Appendix).

of the Hougén–Watson P-Z chart for nuclear matter. We have shown that, knowing the values of a_0 , we can construct all the isotherms on the P-Z chart. The smaller the value of a_0 the higher temperature of nuclear matter is.

In the paper it was shown that during separation of neutrons from atomic nuclei, between Bose-like and Fermi-like regions there exists a nuclear halo related to the chemical potential μ . The properties of halo may be used to model a medium for filtering radioactive elements. Such a filter turned out to be more efficient than the Darcy filtering medium used in the paper [23] (also see [24]).

The obtained in the paper rigorous mathematical approach unexpectedly yields a new picture, which adequately describes the passing to the nuclear matter during separation process of neutrons from atomic nuclei

References

- [1] G. V. Koval' and V. P. Maslov, "Ultrasecond quantization at temperatures distinct from zero," *Math. Notes* **82** (1) 52–57 (2007).
- [2] G. V. Koval' and V. P. Maslov, "Generalization of the Bardeen–Cooper–Schrieffer method for pair interactions," *Teoret. Mat. Fiz.* **154** (3) 495–502 (2008).
- [3] L. D. Landau and E. M. Lifshits, *Statistical Physics* (Fizmatlit, Moscow, 2013).
- [4] V. P. Maslov, *Perturbation Theory and Asymptotical Methods* (Izd. Moskov. Univ., Moscow, 1965; Dunod, Paris, 1972) [in Russian and French].
- [5] A. I. Shtern, "Remark concerning Maslov's theorem on homomorphisms of topological groups," *Russian J. Math. Phys.* **24** (2), 262–262 (2017).
- [6] W.-S. Dai and M. Xie, "Gentile statistics with a large maximum occupation number," *Ann. Phys.* **309**, 295–305 (2004).
- [7] I. A. Kvasnikov, *Thermodynamics and Statistical Physics: Theory of Equilibrium Systems* (URSS, Moscow, 2002), Vol. 2 [in Russian].
- [8] Salo, P. & Hietarinta, J. Ground state in the Faddeev-Skyrme model *Physical review D* **62** 081701(2000).
- [9] Bohr, N. Neutron capture and nucleus structure *Uspekhi Fiz. Nauk* **14** (4), 425–435 (1936).
- [10] Davis, M. & Hersh, R. Nonsrandard analysis *Scienific American* 226 (6), 78–86 (1972).
- [11] Litvinov, G. L. The Maslov dequantization, idempotent and tropical mathematics: a very brief introduction. *Contemp. Math.*, Vol. 377: *Idempotent Mathematics and Mathematical Physics* (Amer. Math. Soc., Providence, RI, 2005).
- [12] Tyurin, N.A. Universal Maslov class of a Bohr-Sommerfeld Lagrangian embedding into a pseudo-Einstein manifold. *Theoretical and Mathematical Physics* **150** (2), 278–287 (2007).
- [13] Yoshioka, A. Maslov's Quantization Conditions for the Bound States of the Hydrogen Atom. *Tokyo J. Math.* **09** (2), 415–437 (1986).

- [14] Czyż, J. On geometric quantization and its connection with the Maslov theory. *Reports of Math. Physics* **15** (1), 57–97 (1979).
- [15] Barilari, D. & Lerario, A. Geometry of Maslov cycles. *Geometric Control Theory and Sub-Riemannian Geometry*. Springer INdAM Series, v.5, 15–35 — (Springer, 2014).
- [16] Borrelli, V. Maslov form and J-volume of totally real immersions. *J. Geom. Phys.* **25** (3–4), 271–290 (1998).
- [17] Littlejohn, R.G. Cyclic evolution in quantum mechanics and the phases of Bohr-Sommerfeld and Maslov. *Phys Rev Lett.* **61**(19), 2159–2162 (1988).
- [18] Chen, B. Y. Maslovian Lagrangian surfaces of constant curvature in complex projective or complex hyperbolic planes *Mathematische Nachrichten* **278** (11), 1242–1281 (2005).
- [19] Maslov, V. P. Thermodynamic Concept of Neutron Separation Energy <https://arxiv.org/abs/1812.02586v4> [physics.gen-ph] (2018).
- [20] Maslov, V. P. Case of less than two degrees of freedom, negative pressure, and the Fermi–Dirac distribution for a hard liquid. *Math. Notes* **98** (1) 138–157 (2015).
- [21] Bruno, A. D. Self-similar solutions and power geometry *Russian Mathematical Surveys* **55** (1), 1–42 (2000).
- [22] Weinstein, A. The Maslov Gerbe *Letters in Mathematical Physics* **69** (1), 3–9 (2004).
- [23] Maslov, V. P., Myasnikov, V. P. & Danilov V. G. *Mathematical Modeling of the Accident Block of Chernobyl Atomic Station* (Nauka, Moscow, 1987) [in Russian].
- [24] Maslov, V. P. On mathematical investigations related to the Chernobyl disaster. *Russian J. Math. Phys.* **25** (3), 309–318 (2018).
- [25] Maslov, V. P. Statistics corresponding to classical thermodynamics. Construction of isotherms, *Russian J. Math. Phys.*, **22** (1), 53–67 (2015).
- [26] Maslov, V. P. Locally ideal liquid *Russian J. Math. Phys.* **22** (3), 361–373 (2015).

Additional information

Competing interests: The author declares no competing interests.

Appendix

Table 1 is based on the IsotopeData which contains 256 stable elements. The table does not include 3 elements: deuterium (by the reason of a computer error), hydrogen-1 (there are no particles to separate), and lithium-3 (separation energy is equal to zero).

Table 1: **Results for isotopes of various chemical elements**

nucleus	B_{nExp}, MeV	a_0	μ_0, MeV	$Z(a_0)$
calcium-40	15.6432	0.0000961785	-144.689	1.10253
silicon-28	17.1798	0.000223074	-144.448	1.11217
molybdenum-92	12.672	0.0000137046	-141.9	1.08548
argon-36	15.2554	0.000134601	-135.975	1.10618
zirconium-90	11.970	0.0000159819	-132.193	1.08662
iron-54	13.3785	0.0000542431	-131.404	1.09686
magnesium-24	16.5311	0.000368113	-130.714	1.1188
strontium-84	11.920	0.0000194398	-129.307	1.08811
krypton-78	12.082	0.0000232997	-128.875	1.08954
sulfur-32	15.0423	0.000191742	-128.753	1.11031
samarium-144	10.520	5.48186*10 ⁻⁶	-127.441	1.07927
selenium-74	12.066	0.0000269819	-126.942	1.09073
yttrium-89	11.474	0.0000176642	-125.57	1.08738
neon-20	16.865	0.00059795	-125.17	1.12599
strontium-86	11.492	0.0000193536	-124.722	1.08808
chromium-50	13.0003	0.0000704205	-124.297	1.09937
tin-112	10.788	0.0000104264	-123.749	1.08353
titanium-46	13.1890	0.0000866761	-123.361	1.10145
cadmium-106	10.874	0.0000119607	-123.242	1.0845
krypton-80	11.521	0.0000235045	-122.795	1.08961
xenon-124	10.483	8.27995*10 ⁻⁶	-122.666	1.08195
barium-130	10.268	7.53057*10 ⁻⁶	-121.131	1.08132
strontium-88	11.113	0.0000192035	-120.689	1.08802
nickel-58	12.217	0.0000517547	-120.57	1.09642
zinc-64	11.862	0.0000414041	-119.712	1.09439
tellurium-120	10.291	9.33055*10 ⁻⁶	-119.197	1.08276
germanium-70	11.534	0.0000338742	-118.716	1.09264
palladium-102	10.568	0.0000139214	-118.177	1.0856
ruthenium-96	10.694	0.000016118	-118.01	1.08668
tin-114	10.299	0.0000107181	-117.859	1.08372

nucleus	B_{nExp} , MeV	a_0	μ_0 , MeV	$Z(a_0)$
cerium-136	9.915	7.05269*10 ⁻⁶	-117.61	1.08089
neodymium-142	9.829	6.36155*10 ⁻⁶	-117.601	1.08022
xenon-126	10.05	8.49544*10 ⁻⁶	-117.317	1.08213
cadmium-108	10.34	0.0000123448	-116.852	1.08472
krypton-82	10.967	0.0000238219	-116.742	1.08972
selenium-76	11.154	0.000028546	-116.719	1.0912
potassium-39	13.078	0.000139344	-116.11	1.10657
cerium-138	9.761	6.95289*10 ⁻⁶	-115.929	1.0808
barium-132	9.822	7.76733*10 ⁻⁶	-115.566	1.08153
chromium-52	12.0394	0.0000717729	-114.88	1.09955
dysprosium-156	9.441	5.26131*10 ⁻⁶	-114.76	1.07902
carbon-12	18.7217	0.00219028	-114.646	1.15006
tellurium-122	9.83	9.60763*10 ⁻⁶	-113.614	1.08296
mercury-196	8.898	3.12117*10 ⁻⁶	-112.802	1.07589
erbium-162	9.20	4.94928*10 ⁻⁶	-112.45	1.07864
bromine-79	10.69	0.0000275384	-112.218	1.0909
ruthenium-98	10.184	0.0000165066	-112.139	1.08686
nickel-60	11.388	0.0000529529	-112.125	1.09663
krypton-84	10.521	0.0000238762	-111.967	1.08974
xenon-128	9.611	8.75246*10 ⁻⁶	-111.926	1.08233
rubidium-85	10.489	0.0000232289	-111.915	1.08952
cadmium-110	9.92	0.0000125732	-111.89	1.08486
praseodymium-141	9.40	6.97794*10 ⁻⁶	-111.567	1.08082
zinc-66	11.059	0.0000427129	-111.266	1.09467
ytterbium-168	9.052	4.60835*10 ⁻⁶	-111.226	1.0782
palladium-104	9.982	0.0000144969	-111.219	1.08589
barium-134	9.468	7.91739*10 ⁻⁶	-111.211	1.08165
germanium-72	10.749	0.0000352147	-110.226	1.09297
dysprosium-158	9.06	5.43981*10 ⁻⁶	-109.769	1.07923
selenium-78	10.498	0.0000293761	-109.548	1.09144
platinum-192	8.666	3.44476*10 ⁻⁶	-109.009	1.07646
cerium-140	9.202	7.3619*10 ⁻⁶	-108.761	1.08117
tin-116	9.563	0.0000115402	-108.733	1.08424
tellurium-124	9.424	9.85452*10 ⁻⁶	-108.635	1.08314
osmium-184	8.665	3.86664*10 ⁻⁶	-107.989	1.07714
erbium-164	8.85	5.10664*10 ⁻⁶	-107.799	1.07883
iron-56	11.197	0.00006593	-107.795	1.09872
chlorine-35	12.6451	0.000199745	-107.717	1.1108
titanium-48	11.6267	0.0000950389	-107.677	1.10241
xenon-130	9.3	8.92282*10 ⁻⁶	-107.614	1.08246
copper-63	10.853	0.0000501121	-107.458	1.09612
mercury-198	8.485	3.28025*10 ⁻⁶	-107.143	1.07617
gadolinium-154	8.895	6.00503*10 ⁻⁶	-106.94	1.07985
barium-136	9.108	8.10141*10 ⁻⁶	-106.774	1.08181
lead-204	8.394	3.07884*10 ⁻⁶	-106.532	1.07581
indium-113	9.44	0.0000126523	-106.516	1.0849
bromine-81	10.157	0.0000279633	-106.488	1.09103
palladium-106	9.561	0.0000147701	-106.346	1.08603
silver-107	9.536	0.0000144582	-106.269	1.08587
ruthenium-100	9.673	0.0000169946	-106.238	1.08708

nucleus	B_{nExp}, MeV	a_0	μ_0, MeV	$Z(a_0)$
antimony-121	9.24	0.0000108769	-105.625	1.08383
iodine-127	9.144	9.69954*10 ⁻⁶	-105.553	1.08303
arsenic-75	10.2	0.0000340779	-105.376	1.09269
tellurium-126	9.114	9.96503*10 ⁻⁶	-104.956	1.08322
platinum-194	8.357	3.55276*10 ⁻⁶	-104.868	1.07664
molybdenum-94	9.678	0.0000201204	-104.651	1.08838
cesium-133	8.986	8.79975*10 ⁻⁶	-104.607	1.08236
krypton-86	9.857	0.0000249209	-104.478	1.09008
germanium-74	10.20	0.0000356351	-104.432	1.09308
oxygen-16	15.6639	0.00129208	-104.189	1.1393
nickel-62	10.596	0.0000545025	-104.029	1.0969
tungsten-180	8.412	4.30616*10 ⁻⁶	-103.936	1.07779
gallium-69	10.313	0.0000424149	-103.831	1.09461
xenon-132	8.937	9.06443*10 ⁻⁶	-103.764	1.08257
tin-120	9.108	0.0000113954	-103.67	1.08415
dysprosium-160	8.576	5.74462*10 ⁻⁶	-103.487	1.07957
ytterbium-170	8.470	4.97246*10 ⁻⁶	-103.432	1.07867
vanadium-51	11.0512	0.0000873841	-103.275	1.10154
selenium-80	9.914	0.0000301155	-103.206	1.09164
erbium-166	8.475	5.29968*10 ⁻⁶	-102.949	1.07906
lanthanum-139	8.778	8.10796*10 ⁻⁶	-102.903	1.08181
palladium-108	9.228	0.0000148746	-102.577	1.08608
rhodium-103	9.3	0.0000166657	-102.524	1.08693
antimony-123	8.965	0.0000109317	-102.419	1.08386
aluminum-27	13.0577	0.000393769	-102.369	1.11975
gadolinium-156	8.536	6.20014*10 ⁻⁶	-102.359	1.08006
lead-206	8.09	3.18599*10 ⁻⁶	-102.352	1.07601
silver-109	9.19	0.0000145974	-102.35	1.08594
scandium-45	11.323	0.000118932	-102.326	1.10481
argon-38	11.8382	0.000177178	-102.263	1.10936
europium-153	8.55	6.51872*10 ⁻⁶	-102.099	1.08038
zinc-68	10.198	0.0000449874	-102.074	1.09514
calcium-42	11.4807	0.000140926	-101.802	1.1067
cadmium-114	9.04	0.0000132641	-101.556	1.08524
titanium-50	10.9392	0.0000939198	-101.44	1.10228
gold-197	8.072	3.60579*10 ⁻⁶	-101.172	1.07673
ruthenium-102	9.220	0.0000174197	-101.028	1.08727
cobalt-59	10.454	0.0000639554	-100.956	1.09843
mercury-200	8.028	3.49222*10 ⁻⁶	-100.875	1.07654
barium-138	8.61	8.53173*10 ⁻⁶	-100.513	1.08215
tin-122	8.813	0.0000114957	-100.237	1.08422
phosphorus-31	12.3116	0.000294229	-100.108	1.11574
hafnium-176	8.165	4.80431*10 ⁻⁶	-99.9881	1.07845
iridium-191	8.027	3.95738*10 ⁻⁶	-99.85	1.07728
calcium-44	11.131	0.000130321	-99.5738	1.10582
tungsten-182	8.065	4.47575*10 ⁻⁶	-99.3332	1.07802
xenon-134	8.552	9.3488*10 ⁻⁶	-99.0376	1.08278

nucleus	B_{nExp}, MeV	a_0	μ_0, MeV	$Z(a_0)$
osmium-188	7.99	$4.162 \cdot 10^{-6}$	-98.9869	1.07758
platinum-196	7.922	$3.76928 \cdot 10^{-6}$	-98.9356	1.07699
molybdenum-96	9.154	0.0000208107	-98.6838	1.08864
thallium-203	7.849	$3.47938 \cdot 10^{-6}$	-98.655	1.07652
dysprosium-162	8.20	$5.97846 \cdot 10^{-6}$	-98.5881	1.07982
samarium-152	8.258	$7.02401 \cdot 10^{-6}$	-97.9872	1.08086
palladium-110	8.814	0.0000152538	-97.7514	1.08627
ruthenium-104	8.901	0.0000174986	-97.5014	1.0873
copper-65	9.911	0.0000534401	-97.4916	1.09672
ytterbium-172	8.019	$5.26548 \cdot 10^{-6}$	-97.4715	1.07902
terbium-159	8.133	$6.37079 \cdot 10^{-6}$	-97.3023	1.08023
thulium-169	8.034	$5.50722 \cdot 10^{-6}$	-97.2836	1.0793
mercury-202	7.754	$3.59707 \cdot 10^{-6}$	-97.1962	1.07671
iridium-193	7.772	$4.05418 \cdot 10^{-6}$	-96.4958	1.07742
osmium-190	7.792	$4.21224 \cdot 10^{-6}$	-96.4479	1.07765
manganese-55	10.2265	0.0000806183	-96.3928	1.10072
tin-124	8.487	0.0000116962	-96.386	1.08434
holmium-165	7.989	$5.93141 \cdot 10^{-6}$	-96.1465	1.07977
iron-58	10.045	0.0000716714	-95.8601	1.09954
thallium-205	7.546	$3.61217 \cdot 10^{-6}$	-94.5614	1.07674
gadolinium-158	7.94	$6.74374 \cdot 10^{-6}$	-94.5088	1.0806
samarium-154	7.967	$7.18682 \cdot 10^{-6}$	-94.3562	1.08101
sulfur-34	11.4171	0.000257572	-94.3534	1.114
nickel-64	9.658	0.0000582298	-94.177	1.09753
rhenium-185	7.667	$4.64917 \cdot 10^{-6}$	-94.1395	1.07825
samarium-150	7.987	$7.68932 \cdot 10^{-6}$	-94.0495	1.08146
platinum-198	7.557	$3.9596 \cdot 10^{-6}$	-93.9995	1.07728
niobium-93	8.831	0.0000240895	-93.9097	1.08981
mercury-204	7.492	$3.70307 \cdot 10^{-6}$	-93.7017	1.07688
erbium-168	7.771	$5.90776 \cdot 10^{-6}$	-93.562	1.07975
europium-151	7.93	$7.63496 \cdot 10^{-6}$	-93.475	1.08141
osmium-192	7.56	$4.30259 \cdot 10^{-6}$	-93.3903	1.07778
xenon-136	8.079	$9.85437 \cdot 10^{-6}$	-93.1351	1.08314
calcium-46	10.394	0.000129101	-93.0811	1.10571
lutetium-175	7.667	$5.40599 \cdot 10^{-6}$	-92.9819	1.07919
molybdenum-98	8.643	0.0000216193	-92.8381	1.08894
gallium-71	9.301	0.0000465095	-92.7903	1.09544
hafnium-178	7.626	$5.20724 \cdot 10^{-6}$	-92.773	1.07895
tantalum-181	7.6	$5.02913 \cdot 10^{-6}$	-92.4372	1.07874
lead-208	7.368	$3.61025 \cdot 10^{-6}$	-92.3333	1.07673
dysprosium-164	7.658	$6.46059 \cdot 10^{-6}$	-91.5116	1.08032
zinc-70	9.218	0.0000490985	-91.4579	1.09593
zirconium-92	8.635	0.0000257533	-91.2439	1.09035
sodium-23	12.4187	0.000677929	-90.6129	1.12799
tungsten-184	7.41	$4.98531 \cdot 10^{-6}$	-90.4886	1.07868
chromium-54	9.7191	0.0000923617	-90.2889	1.10211
ytterbium-174	7.465	$5.73513 \cdot 10^{-6}$	-90.0887	1.07956

nucleus	B_{nExp}, MeV	a_0	μ_0, MeV	$Z(a_0)$
hafnium-180	7.388	$5.31944 \cdot 10^{-6}$	-89.7197	1.07909
gadolinium-160	7.451	$7.22472 \cdot 10^{-6}$	-88.209	1.08105
neodymium-146	7.565	$9.04347 \cdot 10^{-6}$	-87.8583	1.08255
tungsten-186	7.191	$5.08504 \cdot 10^{-6}$	-87.6557	1.07881
strontium-87	8.428	0.0000312581	-87.4262	1.09196
erbium-170	7.257	$6.39635 \cdot 10^{-6}$	-86.7944	1.08026
zirconium-94	8.221	0.0000263225	-86.6924	1.09053
potassium-41	10.0952	0.000187191	-86.6508	1.11002
chlorine-37	10.311	0.000241113	-85.8931	1.11315
neodymium-148	7.333	$9.17055 \cdot 10^{-6}$	-85.0562	1.08264
argon-40	9.8692	0.000208454	-83.6496	1.11133
lead-207	6.738	$4.22995 \cdot 10^{-6}$	-83.3676	1.07768
tin-115	7.546	0.0000174289	-82.6894	1.08727
magnesium-26	11.0931	0.000579398	-82.6825	1.12549
silicon-30	10.6092	0.000415882	-82.5938	1.12053
ytterbium-176	6.9	$6.37343 \cdot 10^{-6}$	-82.1244	1.08023
cerium-142	7.170	0.000010651	-82.0911	1.08368
mercury-199	6.664	$4.79203 \cdot 10^{-6}$	-81.6246	1.07844
sulfur-36	9.8890	0.00027959	-80.9137	1.11507
ruthenium-99	7.464	0.0000267721	-78.5799	1.09067
barium-135	6.972	0.0000128	-78.5475	1.08499
ytterbium-171	6.614	$7.32345 \cdot 10^{-6}$	-78.2126	1.08114
barium-137	6.906	0.0000124904	-77.9682	1.08481
titanium-47	8.8803	0.000158347	-77.7091	1.10804
xenon-129	6.9	0.0000147124	-76.872	1.086
molybdenum-95	7.369	0.0000306275	-76.5911	1.09178
mercury-201	6.231	$5.20344 \cdot 10^{-6}$	-75.8022	1.07895
hafnium-177	6.383	$7.06611 \cdot 10^{-6}$	-75.7085	1.0809
tin-117	6.94	0.0000190653	-75.4559	1.08796
erbium-167	6.436	$8.16677 \cdot 10^{-6}$	-75.4055	1.08186
osmium-187	6.290	$6.23359 \cdot 10^{-6}$	-75.3882	1.08009
palladium-105	7.094	0.0000247645	-75.2409	1.09003
ytterbium-173	6.367	$7.55061 \cdot 10^{-6}$	-75.095	1.08134
dysprosium-161	6.454	$8.98146 \cdot 10^{-6}$	-75.0031	1.0825
krypton-83	7.463	0.0000435172	-74.951	1.09484
cadmium-111	6.98	0.0000218568	-74.8583	1.08903
gadolinium-155	6.435	0.0000100099	-74.0818	1.08325
tungsten-183	6.19	$6.78436 \cdot 10^{-6}$	-73.677	1.08064
zirconium-91	7.194	0.0000358743	-73.6391	1.09313
platinum-195	6.105	$5.84043 \cdot 10^{-6}$	-73.5684	1.07967
gadolinium-157	6.36	$9.85388 \cdot 10^{-6}$	-73.3152	1.08314
xenon-131	6.60	0.0000151871	-73.2805	1.08624
selenium-77	7.419	0.0000540856	-72.8901	1.09683
dysprosium-163	6.27	$9.10368 \cdot 10^{-6}$	-72.7859	1.08259
nickel-61	7.820	0.0000945866	-72.4613	1.10236
hafnium-179	6.099	$7.38282 \cdot 10^{-6}$	-72.0671	1.08119
tellurium-125	6.569	0.0000174216	-71.9821	1.08727

nucleus	B_{nExp}, MeV	a_0	μ_0, MeV	$Z(a_0)$
neon-22	10.3643	0.00105291	-71.0594	1.13551
titanium-49	8.1424	0.000163023	-71.0145	1.10838
ruthenium-101	6.802	0.0000295343	-70.9454	1.09148
chromium-53	7.9391	0.000136538	-70.6496	1.10634
osmium-189	5.92	$6.68448 \cdot 10^{-6}$	-70.5455	1.08054
molybdenum-97	6.821	0.000032856	-70.419	1.09238
tin-119	6.484	0.00002037	-70.0319	1.08848
iron-57	7.6461	0.000118666	-69.1147	1.10478
neodymium-143	6.124	0.0000135297	-68.6489	1.08539
fluorine-19	10.4324	0.00159334	-67.2047	1.14339
sulfur-33	8.6416	0.000450058	-66.5936	1.12168
samarium-149	5.871	0.0000129566	-66.0727	1.08507
zinc-67	7.052	0.0000865705	-65.9715	1.10144
calcium-43	7.9329	0.000245943	-65.9253	1.1134
germanium-73	6.783	0.0000727865	-64.6277	1.09969
neodymium-145	5.755	0.0000144209	-64.1527	1.08585
nitrogen-15	10.8333	0.00298671	-62.9802	1.15714
silicon-29	8.4736	0.00067319	-61.8865	1.12787
helium-4	20.57762	0.0559488	-59.3318	1.26878
nitrogen-14	10.5534	0.00384224	-58.6947	1.16335
boron-11	11.4541	0.00685063	-57.0806	1.17943
magnesium-25	7.3306	0.00132744	-48.5615	1.13981
oxygen-18	8.0440	0.0029541	-46.8529	1.15687
neon-21	6.761	0.00254881	-40.3786	1.15344
boron-10	8.4363	0.0162158	-34.7723	1.20917
carbon-13	4.9463	0.019476	-19.4814	1.21658
lithium-7	7.24997	0.0700691	-19.2724	1.28238
oxygen-17	4.1431	0.0117182	-18.4229	1.19703
lithium-6	5.66341	0.205963	-8.94852	1.36303
beryllium-9	1.6653	0.768153	-0.439262	1.50516